sciendo

ANNALS OF WEST UNIVERSITY OF TIMISOARA PHYSICS
Vol. LXV, 2023

DOI: 10.2478/awutp-2023-0003

STRUCTURAL, MECHANICAL, ELASTIC, ELECTRONIC, MAGNETIC AND OPTICAL PROPERTIES OF SPINEL COMPOUNDS ATi2S4 (A=Ca, Sr AND Ba): AB INITIO STUDY

Mohammed Nadir Bousahla, Mohammed Alaa Bousahla, Abbes Chahed, Zouaoui Bousahla, Habib Rozale, Hadjer Bendjilali

Laboratoire des matériaux et développement durable Djillali Liabès University, Sidi bel Abbes, Algeria

Article Info	Abstract
Received: 15.05.2023 *Accepted: 29.06.2023* **Keywords:***Ab initio, DFT, spinels, structural, elastic, optical.*	This research explored the crystal structure, mechanical and elastic, electronic, magnetic, and optical properties of spinel compoundsATi2S4 (A=Ca, Sr and Ba). The ferromagnetic phase of the compounds was found to be stable, and FP-LAPW method within density functional theory (DFT) was used to calculate and compare the lattice constant a, bulk modulus B0, and its pressure derivative B'. The exchange-correlation potential was also treated with both the GGA and TB-mBJ potential approximation. The results of the study showed that the examined spinels exhibit half-metallic behavior, which makes them a potential material for use in spintronic and optoelectronic devices.

1. Introduction

The remarkable attributes of ternary spinel sulfides have garnered considerable attention from scientists because of their desirable characteristics [1-2]. These types of sulfides possess the properties of being ferromagnetic materials that allow for simultaneous modulation, making them attractive to researchers exploring their potential use in emerging spintronic devices [3]. The general formula for these materials is A2XB4, where A and X represent cations and B represents anions. They typically belong to the space group 227 (Fd3m) and have a cubic symmetry.

The scientific community has not studied these materials in detail according to the latest literature review [4].

In this research, the magneto-electronic properties of our compounds were calculated, with a goal of exploring their suitability for use in spintronic. The study revealed the potential of these materials to be used in this field. Additionally, the transport properties of the spinels under investigation were analyzed to assess their suitability for utilization in thermoelectric applications. The study sought to determine whether these properties make them relevant for such purposes. Using the theory of density functional (DFT) [5] in accordance with the full-potential linearized augmented plane wave (FP-LAPW) approach, we have examined A2XB4 dynamic spinel sulfides to investigate their structural, electronic, mechanical and elastic, magnetic and optical properties. The properties of these materials, such as strength and flexibility, have the potential to revolutionize industries such as manufacturing and construction. This research provides a deeper understanding of the fundamental principles behind material properties, which can lead to even further innovation in the field. Moreover, this work contributes to our general knowledge about materials science by providing more information on how specific mechanical and physical properties are related to unique structural configurations at the molecular level. These insights can be used in other areas of scientific inquiry beyond material science. Furthermore, this study could potentially have far-reaching impacts on society. By developing stronger and more flexible materials that can withstand

2. Simulation technics

The ability to run the computations detailed in this analysis was made more feasible because of the inexpensive nature of utilizing the wien2k computational code [6]. The code operates under the theory of density functional [5], and to optimize the geometrical structure and minimize total energy in this study, the PBE GGA [7] method is employed. Through the optimization of geometrical structure and minimization of total energy parameters. The study identified and utilized the specific molecular and electronic properties of materials that exhibit high coherence, and with modified methods based on a Becke-Johnson potential, we were able to accurately approximate intrinsic properties such as band gaps. [8-9]. The Boltzmann transport theory, which is incorporated into the Boltztrap algorithm [10] was used to model the thermoelectric characteristics. Using data from DFT computations as input, the BoltzTraP tool was used to examine the transport characteristics. The potential at the surface of the sphere MT was kept continuous, and the potential and charge density shape were formed without

approximation, according to the FP-LAPW approach. The analyzed materials exhibit complex structures with various regions of different density and characteristics. To handle such complexity, a modeling approach based on lattice harmonics inside atomic spheres and Fourier series in the interstitial regions was employed. This method involves expanding the wave functions of the constituent atoms in both regions separately and then combining them to obtain the overall wave function of the material.

3. Structural Properties

Cubic spinel sulphides ATi2S4 with stable ternary structures and are classified in the Fd-3m space group. The positions of A, Ti and S atoms in the spinel structure (0.125, 0.125, 0.125), (0.5, 0, 0), and (0.2539, 0.2539, 0.2539)/(0.2545, 0.2545, 0.2545), respectively. In order to determine the fundamental properties of our compounds, their respective total energies were calculated at various volumes and then fitted by the state equation of Murnaghan [11]. The table below provides data on several specific characteristics of three materials, namely CaTi2S4, SrTi2S4, and BaTi2S4. These characteristics include the lattice parameter a, optimized volume V, bulk modulus B, and the first-order derivative B', which have all been calculated for the non-magnetic (NM) and ferromagnetic (FM) orderings of the materials' relaxed structures, we avoided the calculation of antiferromagnetic phase because it may not be of interest for our research question being investigated and even some similar research found that these compounds are stable in the ferromagnetic phase [12]. These calculations were performed with the aim of understanding the composition and properties of these materials more deeply, and may have implications for their potential use in various technological applications. The FM phase CaTi2S4 (-15940.34 Ry), SrTi2S4 (-25937.86 Ry) and FM phase of BaTi2S4 (-45775.69 Ry) have the minimum unit cell volume. In the case of CaTi2S4 and BaTi2S4, B drops when the IIA metals cations swaps from Ca to Sr to Ba. The values of a_0 for the three compounds show an increasing trend: a_0 (CaTi2S4) < a_0 (SrTi2S4) < a_0 (BaTi2S4). Ti and S atoms are the same for the three compounds, where r(Ti) = 2.0 Å and r(S) = 1.9 Å, these values refer to the muffin-tin radii of the respective atoms, which are used within the context of the muffin-tin approximation method for calculating electronic structures of materials. In this approximation method, the atoms are treated as individual spheres (muffin-tin spheres) that are centered at the atomic sites and overlap with each other. The obtained results can be well explained by the ionic radii of both Ti and S: the lattice parameter value is found to increase with the increasing size of A atom involved in the ATi2S4. The relationship between the values of bulk modulus 'B' and a_0 indicates an inverse inverse trend, which mean

that the compounds is more rigid from CaTi2S4 to BaTi2S4, which aligns with the familiar relationship between bulk modulus and volume, denoted as B∝ V^{-1}.

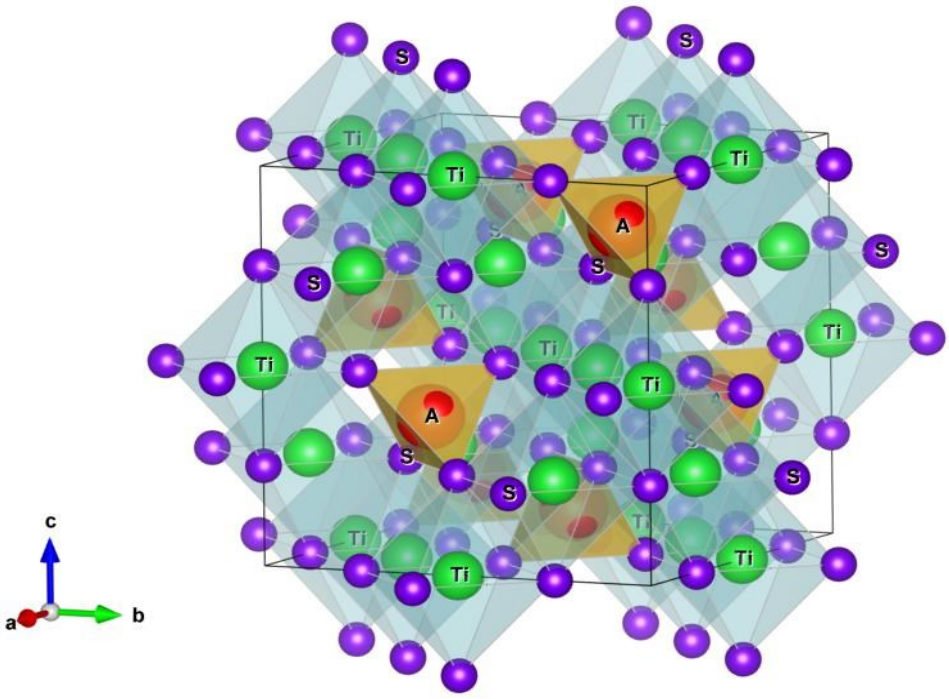

Figure 1. Schematic illustration of ATi2S4 spinel compounds

Table 1. Lattice parameter, bulk modulus , its derivative and optimized volume of $CaTi_2S_4$, $SrTi_2S_4$ and $BaTi_2S_4$, calculated with PBE-GGA approximation.

Compounds	*Energy (Ryd) NM phase*	*Energy (Ryd) FM phase*	*a* (Å)	*B(GPa)*	$V(u.a)^3$	*B'*
$CaTi_2S_4$	-15939.73	-15940.34	10.79 10.73[a]	67.07 65,38[a]	2121.85	3.35
$SrTi_2S_4$	-25937.79	-25937.86	11.15	57.48	2338.02	4.68
$BaTi_2S_4$	-45774.19	-45775.69	11.48	45.75	2567.32	3.28

[a]Ref [4]

4. Mechanical and elastic properties

These results were made with wien2k code using IRelast package [13]. Understanding the elastic properties of materials, particularly their elastic constants, is essential for analyzing the mechanical stability of solids in response to different strains. The mechanical strength of materials is greatly influenced by their elasticity properties. Therefore, a thorough knowledge

of these properties is important in understanding how forces can impact the integrity and durability of solids. the elastic properties and mechanical characteristics of three different spinels (CaTi2S4, SrTi2S4, and BaTi2S4) were examined. Specifically, the elastic parameters of these spinels were calculated by analyzing the energy associated with tetragonal and rhombohedral pressure [14]. For materials that exhibit cubic symmetry, the Born stability criteria [15] require three specific elastic constants, namely C11, C12, and C44, in order to be met. This is a widely accepted condition in determining stability. These conditions require that C_{11}, C_{44}, C_{11}- C_{12}, C_{11} + 2 C_{12}, and C_{12} < C_{11} are all greater than zero. It is vital to utilize the Voigt-Reuss-Hill approximations [16] to calculate the bulk modulus B and shear modulus G, as this is essential in determining a multitude of mechanical properties for materials. These calculations are important for understanding how a material will respond to forces applied to it. As a result, the precise determination of a material's bulk modulus and shear modulus is crucial in anticipating how it will react under various conditions. This, in turn, can substantially enhance our capacity to assess and analyze the material's mechanical characteristics. B is determined as the average of BV and BR, whereas BV and BR are both calculated as (C_{11} + 2 C_{12})/3. GR is computed as 5C44 (C_{11} C_{12}) / (4 C_{44} + 3 C_{11} - C_{12}) and GV is calculated as (C_{11} C_{12} + 3 C_{44}) /5. After that, Young's modulus E and Poisson's ratio *v* were calculated using GV and GR. A was calculated as 2 C_{44} / (C_{11}+ C_{12}), which is the Zener anisotropy factor. In the table below, the mechanical characteristics and elastic constants of three spinel compounds (CaTi2S4, SrTi2S4 and BaTi2S4) at (0 K, 0 GPa) are presented. By accurately calculating these values, researchers can assess the mechanical properties of the material and predict how it will behave under various conditions, thus improving our understanding of its overall mechanical behavior. By comparing the results obtained with the ones from previously established data, the accuracy and reliability of the computed elastic properties can be validated. For instance, when using the bulk modulus B for this purpose, the derived values were found to correspond to those in Table 1, as shown in Table 2. Therefore, these findings suggest that the computed mechanical characteristics can be considered reliable.

The Young's modulus (E) calculations show that the three spinel compounds are ductile. Furthermore, calculated values of Poisson's ratio (v), Pugh's ratio (B/G), and Cauchy pressure ($C_p = C_{12}-C_{44}$) [17] support the ductile nature of CaTi2S4, SrTi2S4, and BaTi2S4. Notably, the computed Zener's anisotropy factor A for these compounds is greater than 1 [18], indicating isotropy, which is different from the case of anisotropic materials.

5. Electronic properties

Table 2. Elastic constants C_{11}, C_{12}, C_{44} (GPa), Bulk modulus B (GPa), Voigt Modulus GR (GPa), Reuss Modulus GR(GPa), Shear Modulus G (GPa), Young's modulus E (GPa), Poisson's ratio v, Pugh's ratio (B/G), Cauchy's pressure (Cp = C_{12}- C_{44}), Zener anisotropy factor A.

Compounds	C11	C12	C44	B	G	E	v	B/G	Cp	A
CaTi2S4	69.38	64.01	56.60	65.80	19.58	49.02	0.25	3.35	7.40	0.84
SrTi2S4	70.26	65.01	54.51	66.76	18.84	51.67	0.37	3.54	10.49	0.81
BaTi2S4	71.12	66.01	53.64	67.71	18.11	49.90	0.377	3.73	12.37	0.78

Specifically, the band structures and state densities of CaTi2S4, SrTi2S4, and BaTi2S4 in the cubic phase. The PBE-GGA model was used to determine the structural optimization of the cubic phase, while the electronic structure was computed using DFT-based mBJ-GGA approximation [19], which corrects the bandgap without affecting the structural optimization. A thorough understanding of electronic characteristics is important for evaluating materials for use in optoelectronic devices Fig. 2 shows band structure plots for spinels in both spin directions, derived using mBJ and PBE-GGA. The spin down BS exhibit a band gap around the Fermi level, while spin up BS display a metallic nature. The sulfides studied here exhibit an almost half-metallic ferromagnetic nature. Comparisons were made between mBJ-GGA and PBE-GGA to evaluate the band gap.For CaTi2S4, the band structure plots show a direct gap for both spin up and down. However, it has been observed that the plots corresponding to SrTi2S4 and BaTi2S4 exhibit an indirect gap, as the valence band maxima occur at the X symmetry point, and the conduction band minima occur at Γ symmetry point. In comparison to various other methods, the GGA approximation yields lower values for gap energy. To address this issue, the mBJ-GGA method is frequently implemented to correct for this underestimation. The band gap for various materials is provided in figures 2-3-4. According to these figures, CaTi2S4 has a direct gap of 1.9438 (spin down) eV when utilizing the mBJ GGA functional, whereas BaTi2S4 exhibits an indirect gap of 1.49 (spin down) eV. The energy necessary for electron transitions between the valence and conduction bands differs for BaTi2S4 and CaTi2S4. Specifically, in BaTi2S4, a transition requires an energy of 1.49 eV, whereas in CaTi2S4, a spin-down electron necessitates 1.9438 eV for a direct transition.

Understanding these differences in required energy is important for studying the electronic properties of materials and their behavior under various conditions.

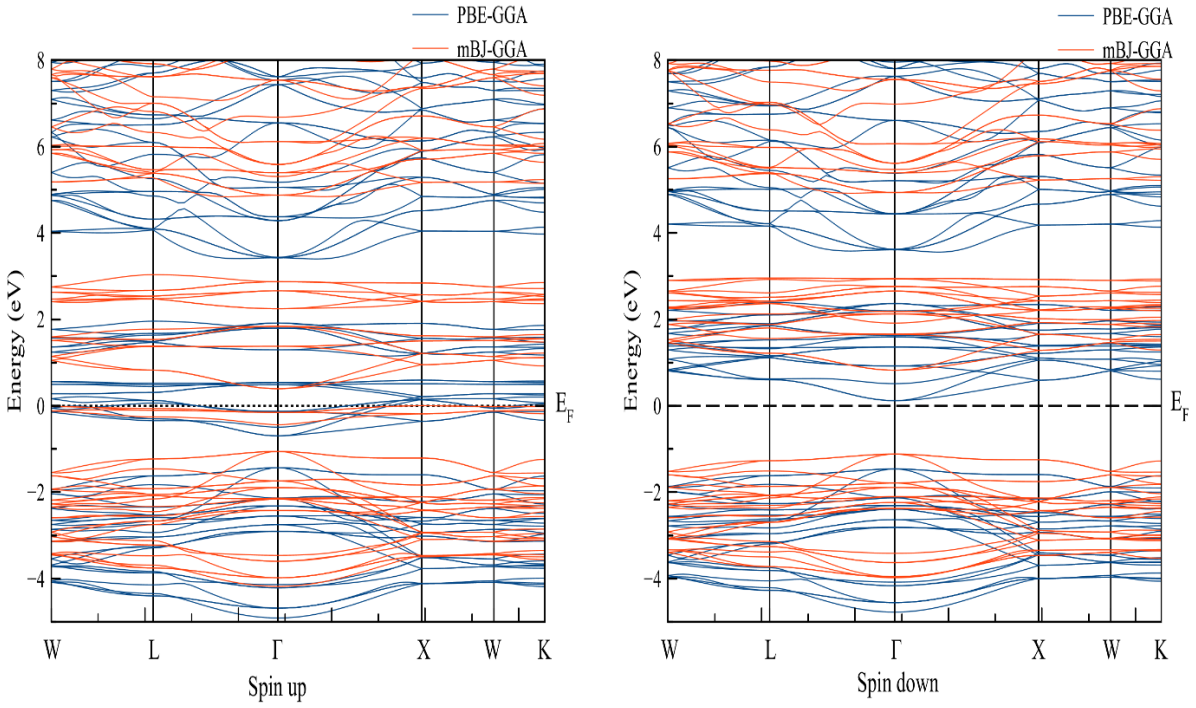

Figure 2. Band structure plots of CaTi2S for both spin up and down respectively using PBE GGA and mBJ GGA approximations.

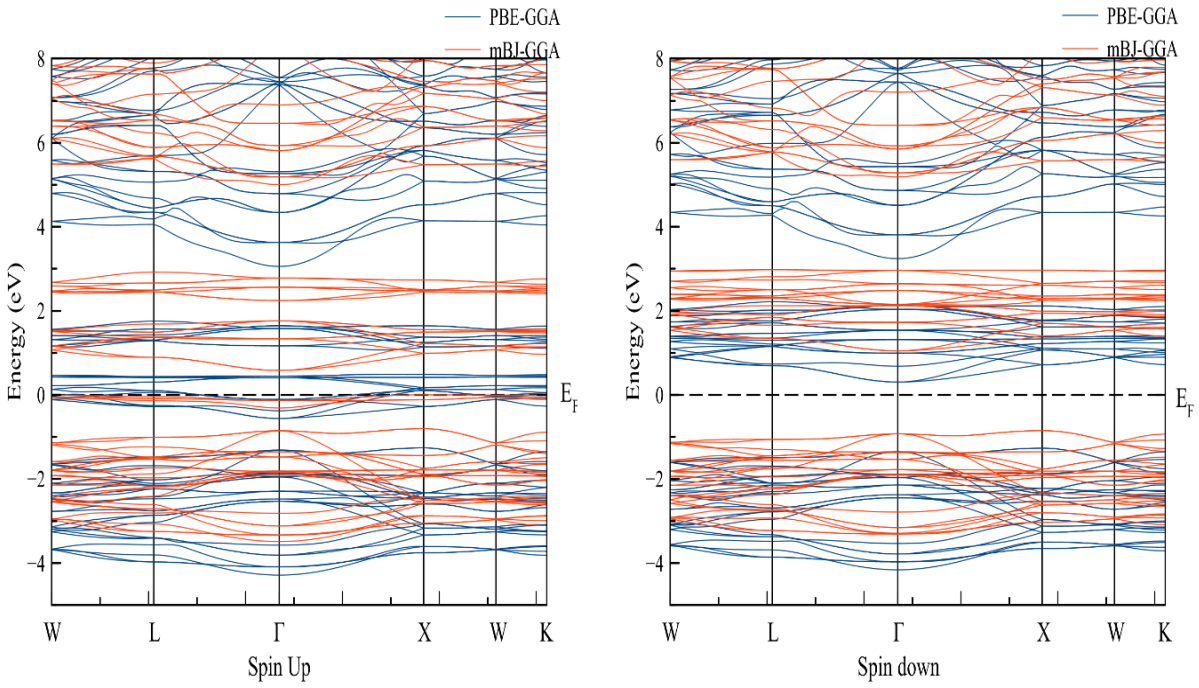

Figure 3. Band structure plots of SrTi2S4 for both spin up and down using PBE GGAand mBJ GGA approximations.

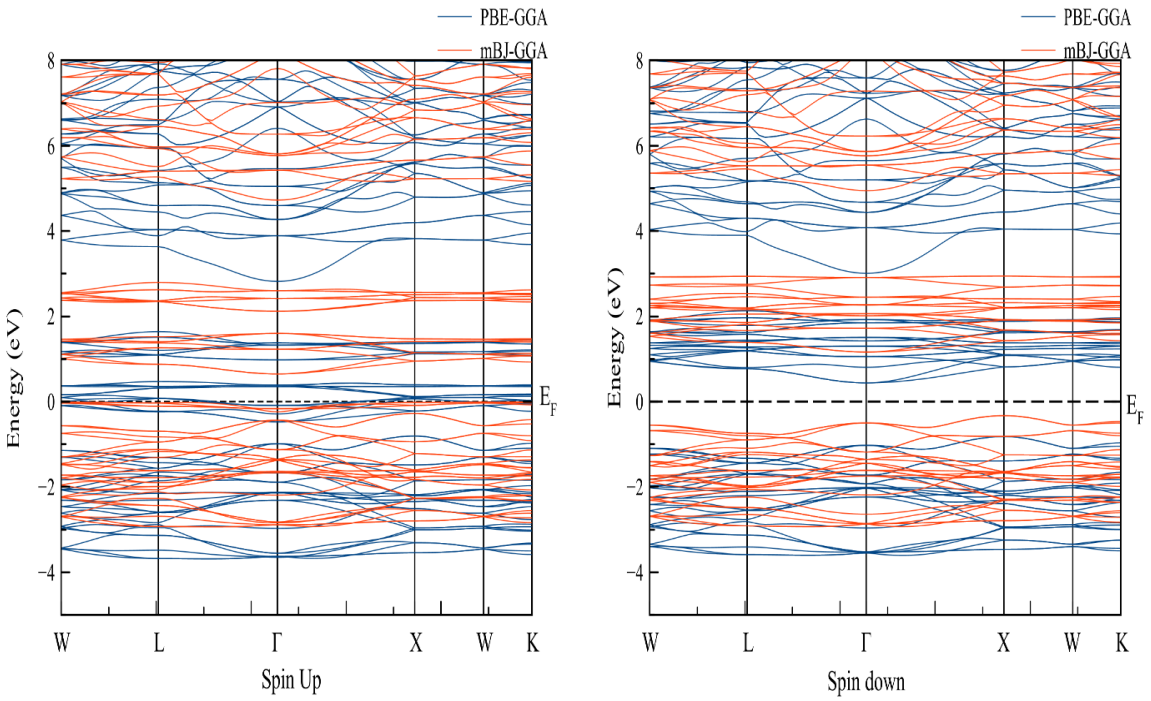

Figure 4. Band structure plots of BaTi2S for both spin up and down using PBE GGA and mBJ GGA approximations

In order to acquire a more profound comprehension of the electronic properties of CaTi2S4, SrTi2S4, and BaTi2S4, their total and partial density of states (DOS) were analyzed using mBJ-GGA. The findings are consistent with previously reported results [20], indicating that all three materials exhibit semiconductor behavior, with an energy gap surrounding the Fermi level for the minority spin DOS. Meanwhile, for the majority spins, a DOS peak is observed at the Fermi level, demonstrating their metallic character. This feature results in the Fermi level displaying a complete 100% spin polarization for the three compounds illustrated in Figure 5-6-7as evidenced by their respective calculated DOS.

For CaTi2S4, The DOS reveals that the valence band in the energy range (–4.2 to –0.99eV) for spin up and (-4.04 to -1.02) for spin down under the Fermi level comes from a strong hybridization of states of the two atoms S and Ti while the contribution of Ca atoms are negligible. The upper band in the energy range of (-0.5 to 0.06) for spin up is characterized by the hybridization of the eg states of Ti and p states of S atomic orbitals, the d and p states of Ti and S respectively cause strong p-d hybridization, a minor contribution from Ca atoms is also present in this region. In the energy range (0.33 to 3.11) for spin up and (0.74 to 3.02) for spin down which is the conduction band (above the Fermi level is basically dominated by the d-states of Ti as well as the states of S with a small contribution of Ca atoms. The DOS for

SrTi2S4 suggests that the valence band below the Fermi level in the energy range (-3.55 to -0.72eV) for spin up and (-3.36 to -0.78) for spin down originates from a significant hybridization of states of the two atoms S and Ti, with Sr atoms contributing negligibly. The hybridization of the eg states of Ti and p states of S atomic orbitals defines the top band for spin up. The d and p states of Ti and S cause strong p-d hybridization, and a little contribution from Sr atoms is also present in this area. The conduction band has an energy range of (0.52 to 3.00) for spin up and (0.98 to 3.05) for spin down (above the Fermi level).

The DOS for BaTi2S4 indicates that the valence band in the energy range (-3.00 to -0.64eV) for spin up and (-3.00 to -0.26) for spin down under the Fermi level results from a substantial hybridization of states of the two atoms S and Ti, with Ba atoms contributing negligibly. The top band for spin up is defined by the hybridization of the eg states of Ti and p states of S atomic orbitals, the d and p states of Ti and S cause significant p-d hybridization, and a little contribution from Ba atoms is also present in this area. In the energy range (0.5 to 2.86) for spin up and (1.09 to 3.00) for spin down, which is the conduction band (above the Fermi level), the d states of Ti and S are primarily dominant, with a little contribution from Ba atoms.

6. Magnetic Properties

To understand the interest of spin electronics technology, we must check the magnetic properties of materials. Spintronic consider both charge and spin in the movement of conduction electrons [21,22]. According to the relationship below, the magnetic moment caused by a material's spin is determined by the difference between the total occupation numbers of the majority and minority spin orbitals. Specifically, the spin magnetic moment μ is defined as this formula [23]:

$$\mu=\sqrt{n(n+2)}$$

where n= Number of unpaired electrons.

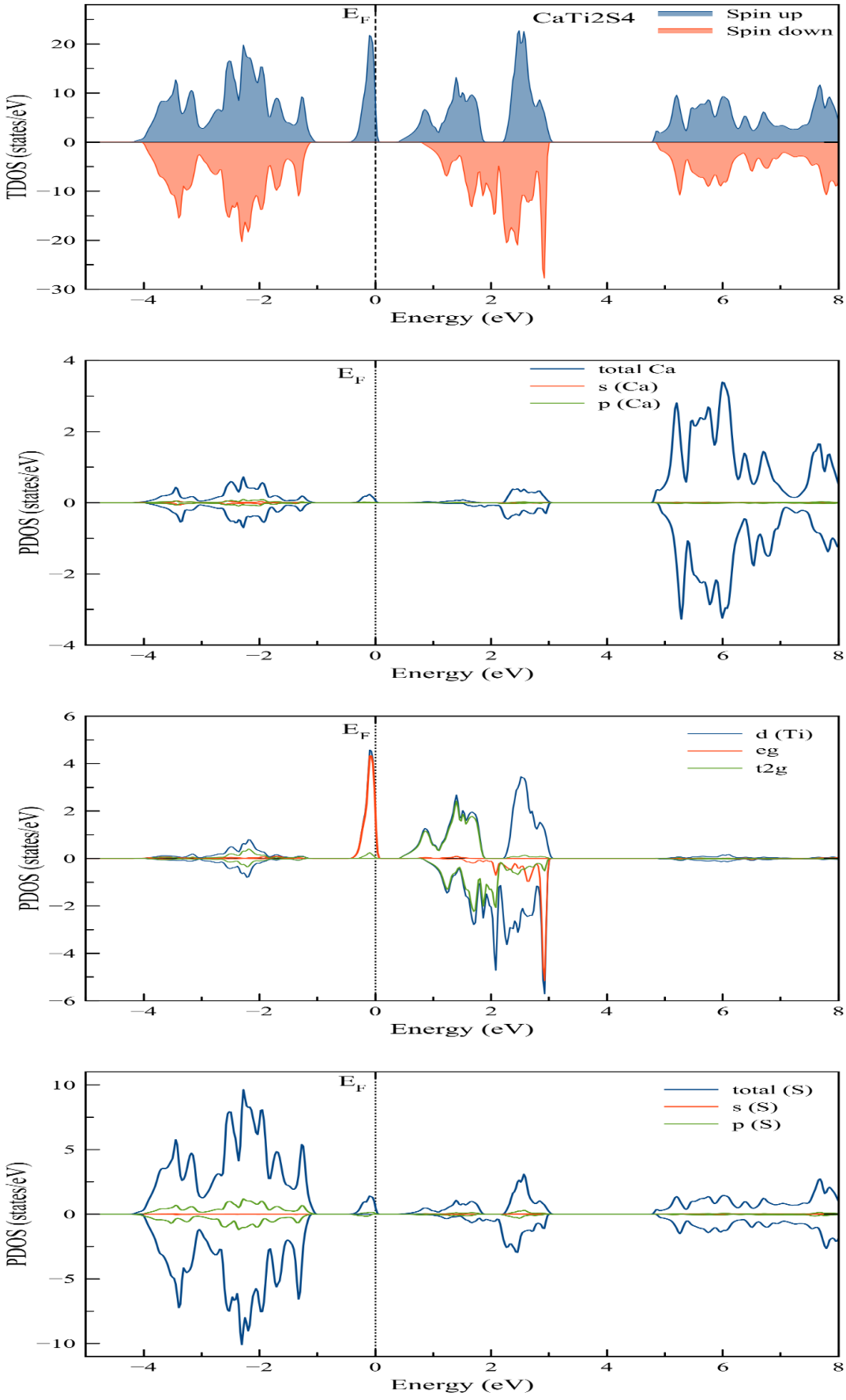

Figure 5. Total and partial DOS of CaTi2S4

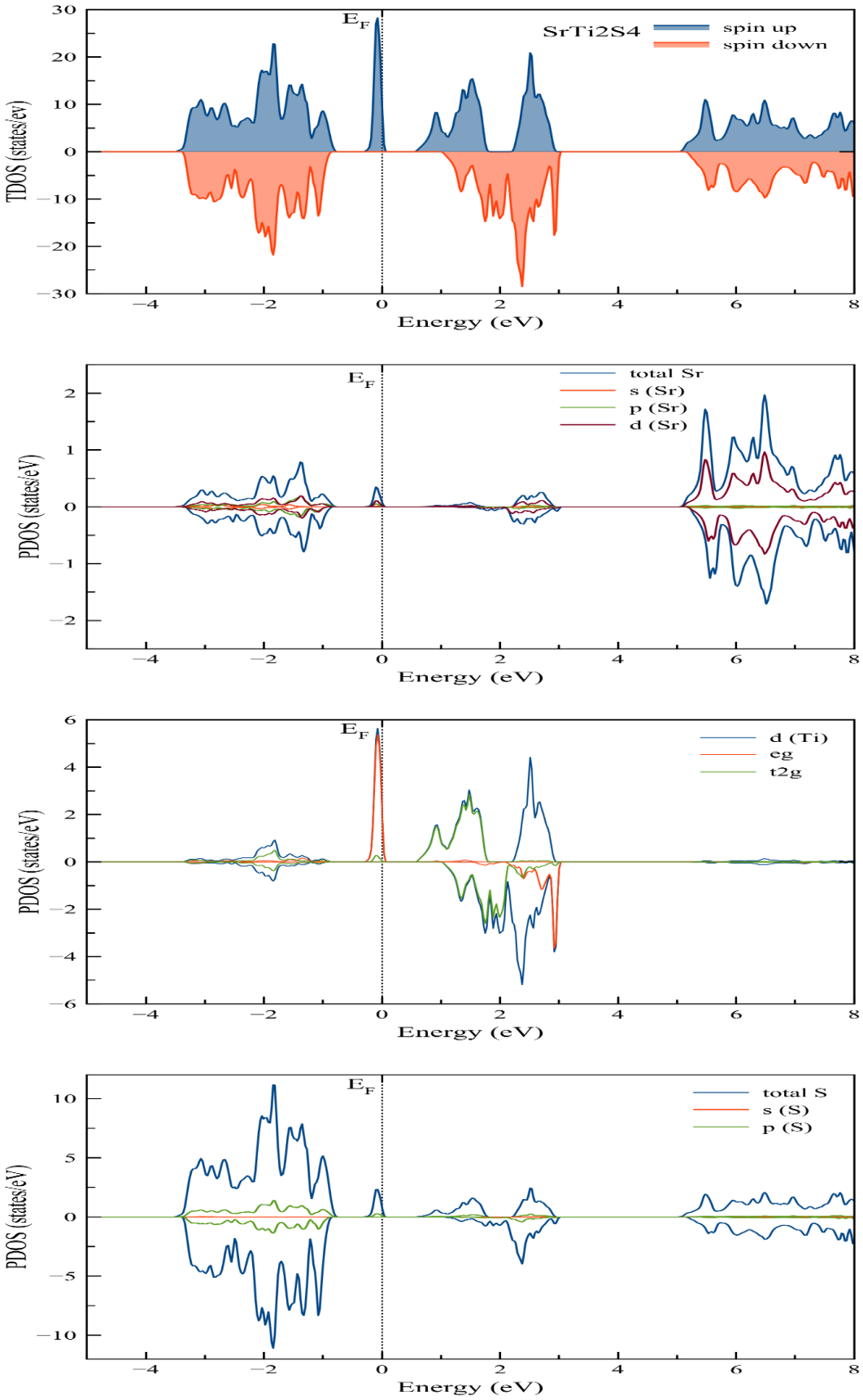

Figure 6. Total and partial DOS of SrTi2S4

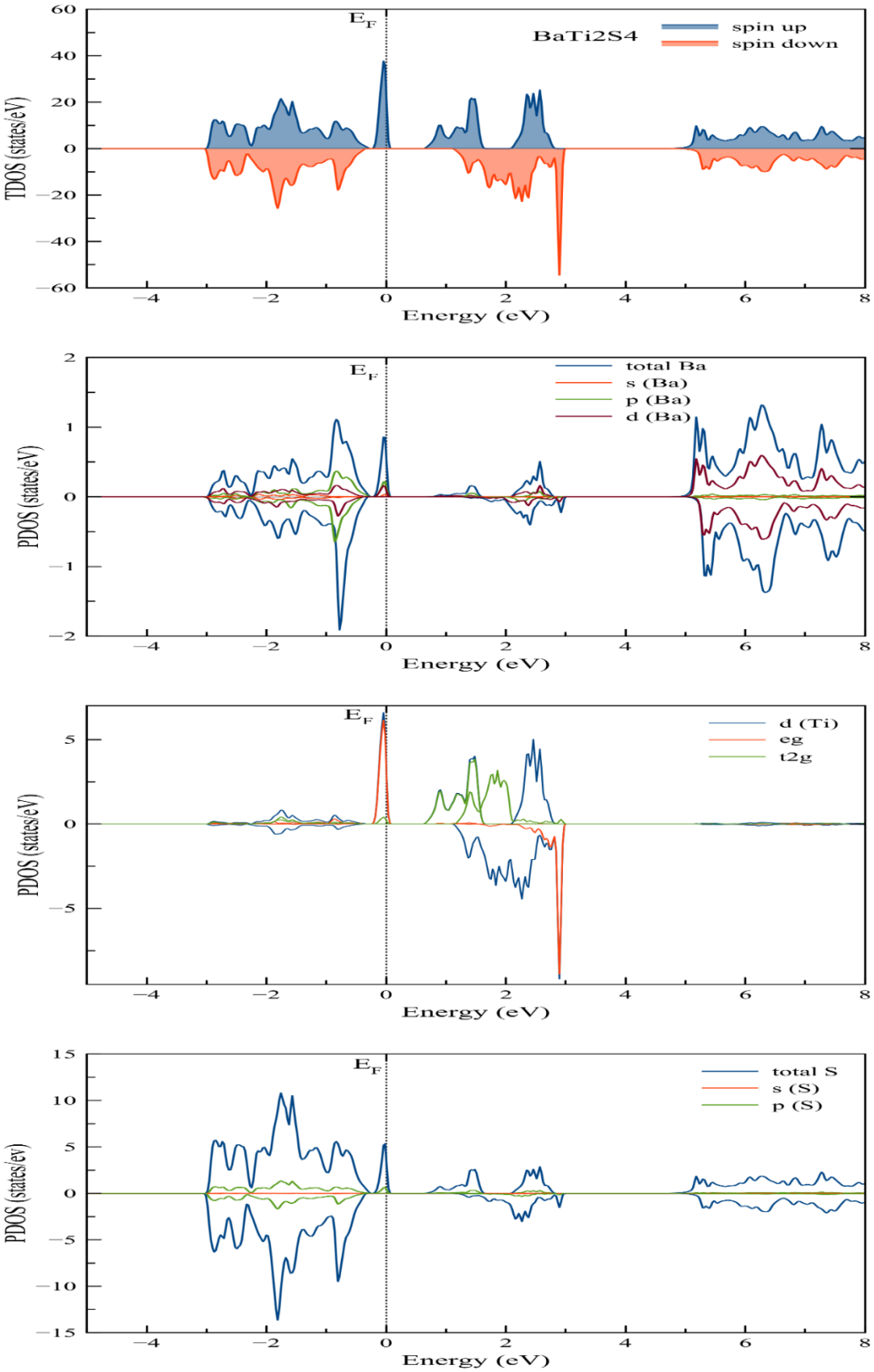

Figure 7. Total and partial DOS of BaTi2S4

Spinels have a wide range of behavior, from metallic or half-metallic behavior to semiconducting behavior. Their magnetic properties are of a particular interest due to their unfilled 3d orbitals [24]. Our calculations yielded the total and partial magnetic moment for three compounds - CaTi2S4, SrTi2S4, and BaTi2S4 - in both interstitial and spheric regions. We can gain a better understanding of their overall behavior. This information can be helpful for a variety of applications, such as designing new materials with desired magnetic properties or predicting how these compounds will behave in different environments. The magnetic moment of CaTi2S4 primarily originates from its titanium atoms. Specifically, the Ti atoms contribute a magnetic moment with a value of M (Ti)= 0.92168 μ_B, while the S atom has negligible moment M (S)= -0.01810 μ_B and M(Ca)=0.01744 μ_B.

The largest contribution to the overall moment of SrTi2S4 is attributed to the titanium (Ti) atom, with M(Ti)=0.94320 μ_B, while the S atom contributes less, with M(S)=-0.02995 μ_B and M(Sr)= 0.01106 μ_B.

The total moment of BaTi2S4 is mostly derived from the Ti atom with a value of M(Ti)=0.96747 μ_B while of the S atom is small M(S)=-0.02995 μ_B and M(Ba)= 0.00641 μ_B.

The substantial moment of the Ti atom can primarily be attributed to the significant exchange observed in Ti-3d states. There is a noticeable contrast in the majority and minority spin graphs in relation to this transaction, qualitatively explaining the moment of the Ti atom. However, the same cannot be said of other s, p, and d states of Ca and Ba atoms. Compared to titanium (Ti), the local magnetic moment of these elements is relatively low, which results from the absence of any significant asymmetry between the spin-up and spin-down curves. The quantitative results of the different magnetic moments are summarized in table 3.

Table 3. Magnetic moments of ATi_2 S_4 (A= Ca, Sr and Ba) spinels.

	M (A)	**M (Ti)**	**M (S)**	**M_{int}**	**M_{tot}**
CaTi2S4	0.017 0.010[a]	0.921 2.04[a]	-0.00986 0.075[a]	0.357 0.42[a]	8 8[a]
SrTi2S4	0.011	0.943	-0.018	0.349	8
BaTi2S4	0.006	0.967	-0.029	0.357	8

[a]Ref [4]

7. Optical properties

To investigate the optoelectronic properties of spin-polarized systems in Wien2k, one typically performs calculations of the dielectric function and optical conductivity tensor under the spin-polarized constraint. The calculations include calculating the spin-resolved electronic states and solving the corresponding spin-dependent Kubo-Greenwood equation [25]. The way that matter interacts with light can be understood through the complex dielectric function. This function contains real and imaginary parts that can be utilized to determine various optical properties, including absorption coefficient and refractive index. It provides insight into how a waveform will interact within a material. The dielectric function of a material is often represented as the sum of its real and imaginary parts: $\varepsilon(\omega) = \varepsilon_1(\omega) + \varepsilon_2(\omega)$ [26]. The real component, ε_1 (ω), describes the electronic polarizability of the material, while the imaginary component, ε_2 (ω), provides information about its absorption behavior. This allows for calculation of various optical properties, such as the refractive index and absorption coefficient. The presence of magnetic fields can be detected based on this specific function. Half-metals are able to act as conductors for one spin channel while functioning as semiconductors for the opposite spin channel. Due to this unique characteristic, charge carriers are only able to conduct electricity in one direction for half-metallic materials, resulting in 100% spin polarization and the generation of spin-polarized current that enhances the effectiveness of magnetoelectronic devices. Spinel compounds demonstrate remarkable magnetic and optical properties, and can serve as electrical switches since they possess only one type of electron, either spin-up or spin-down. Thanks to these special features, half-metals are well-suited for a range of spintronic applications [27].

The role of material optical properties is becoming increasingly significant in the field of technology. The impact of the interplay between matter and electromagnetic radiation is of utmost importance in determining various properties. These properties are influenced by a multitude of factors, including the radiation wavelength and frequency. In addition, material characteristics including refractive index, dielectric constant, and band gap values also impact the interaction. Understanding these properties can be useful in anticipating how light will behave within different materials.

Tunable optical properties of materials are finding increasing applications in fields ranging from biosensing to photovoltaics. This research focuses on investigating the optical response of the spinel compounds ATi2S4 (A = Ca, Sr and Ba); Figure 9 highlights our findings by displaying the real component ε_1 (ω) of the dielectric function $\varepsilon(\omega)$ for our compounds. Our

data shows that these compounds possess a static dielectric constant ε_1 (0) of 7.53, 7.27, and 8.08 for CaTi2S4, SrTi2S4, and BaTi2S4, respectively. The research highlights the potential uses of these materials in diverse technological applications. Notably, the value of ε_1 (0) increases as the band gap decreases (Eg (Ba)< Eg(Sr)< Eg (Ca)), in agreement with Penn's approach [28], which relates the inverse relationship between ε_1 (0) and Eg.

$$\varepsilon_1 (0) \approx 1 + (\hbar\omega p/\mathrm{Eg})^2$$

The behavior of materials can be influenced by parameters like ωp and Eg, where ωp is the plasma frequency and Eg is the energy band gap. By analyzing the real component ε_1 (ω) of the dielectric function for CaTi2S4, SrTi2S4, and BaTi2S4, we found that these compounds have maximum values of 8.39 at 0.77 eV, 8.36 at 3.19 eV, and 9.54 at 1.23 eV, respectively. These values suggest that the compounds' behavior can be fine-tuned for specific applications in different technological fields. The observation that the real component ($\varepsilon 1$ (ω)) of certain materials can take on negative values and result in the reflection of all incident electromagnetic waves is relevant to the goals of our manuscript. Specifically, our aim was to characterize the optical properties of certain spinel compounds and investigate the effect of various factors, such as crystal structure and chemical composition, on their optical behavior. The results we presented, which showed negative values of $\varepsilon 1$ (ω) for certain energy ranges in the three studied spinel compounds (CaTi2S4, SrTi2S4, and BaTi2S4), suggest that these materials exhibit strong absorption of incident electromagnetic waves in those regions. This absorption can be attributed to the presence of certain electronic states or energy bands within the materials that are able to interact with the incident light and absorb its energy. Furthermore, the observation that the negative values of $\varepsilon 1$ (ω) result in the complete reflection of all incident electromagnetic waves indicates that these materials may have potential applications in certain optical devices, such as mirrors or reflectors. Overall, these findings contribute to a better understanding of the optical properties of the studied spinel compounds and may have implications for future research or technology development in this area. The imaginary component ε_2 (ω) of the dielectric function $\varepsilon(\omega)$ is displayed in Figure 9, with maximum values of 9.06 at 4.20 eV for CaTi2S4, 9.95 at 3.90 eV for SrTi2S4, and 9.99 at 3.06 eV for BaTi2S4, indicating a bandgap-dependent behavior. The static component of reflectivity R(ω), or zero-frequency reflectivity R(0), was found to be 21.70%, 21.08.28%, and 23.01% for CaTi2S4, SrTi2S4, and BaTi2S4, respectively, as shown in Fig.12. Additionally, maximum reflectivity

R(ω) was observed between 9 eV to 13.5 eV, which matches the negative ε_1 (ω) values of the three compounds, indicating their potential use as Bragg's reflector [29]. Our results suggest the possibility of tuning the optical properties of these compounds to match specific application requirements.

The absorption coefficient of the spinels compound ATi2S4 (A=Ca, Sr, Ba) changes based on energy levels. This information is presented in Figure 10 included in the paragraph. In the visible energy range, the absorption spectrum of all three materials displays a solitary absorption band that initiates at their individual band gap. Over the studied energy range, this band subsequently expands to cover a region of approximately 4 eV in width.

The frequency-dependent refractive index n (ω) of the three materials was calculated and is presented in Fig. 11. To obtain the static refractive index n (0), we used an equation that involves the static dielectric constant: $n(0) = \sqrt{\varepsilon_1}(0)$. The calculated values of n (0) can provide insight into the behavior of the materials at zero frequency and could be useful in designing applications that require a well-defined refractive index. CaTi2S4, SrTi2S4 and BaTi2S4 have values of 2.75, 2.70 and 2.84, respectively.

The behavior of the refractive index n (ω) was studied for CaTi2S4, SrTi2S and BaTi2S4, and it was observed that n (ω) increases as the energy increases.In the case of the studied materials, Eg values were obtained by analyzing the corresponding spectra. The results show that the peaks with the lowest energy correspond to the materials with the highest Eg, following the pattern Eg (Ca) > Eg (Sr) > Eg (Ba). This finding suggests that the band gap of these materials decreases as the atomic radius of the cation increases These results have valuable implications for the design of materials with specific optical properties, like refractive index and band gap, to match distinct application requirements.

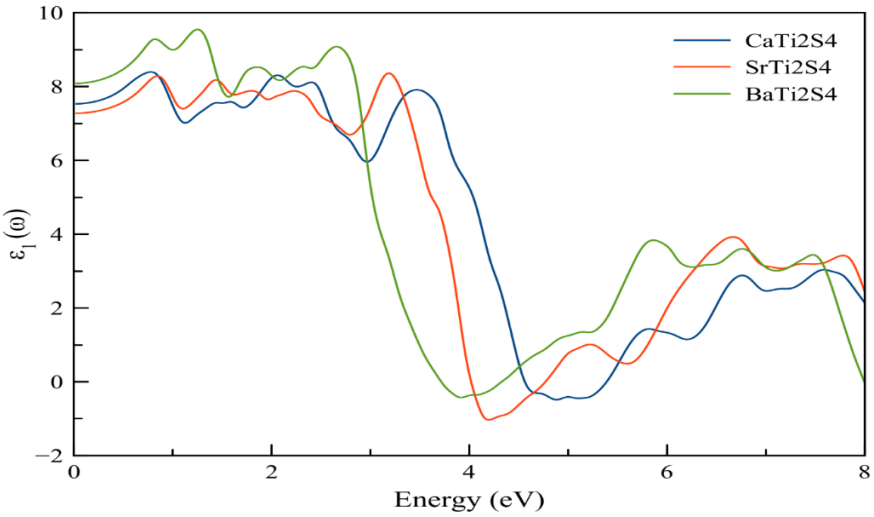

Figure 8. Calculated dielectric function: real part of ATi2S4 (A = Ca, Sr and Ba)

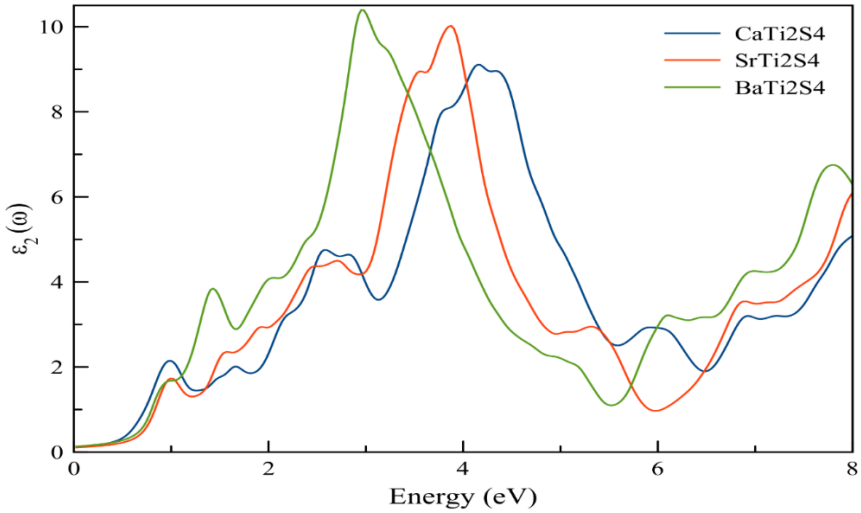

Figure 9: Calculated dielectric function: imaginary part of ATi2S4 (A = Ca, Sr and Ba)

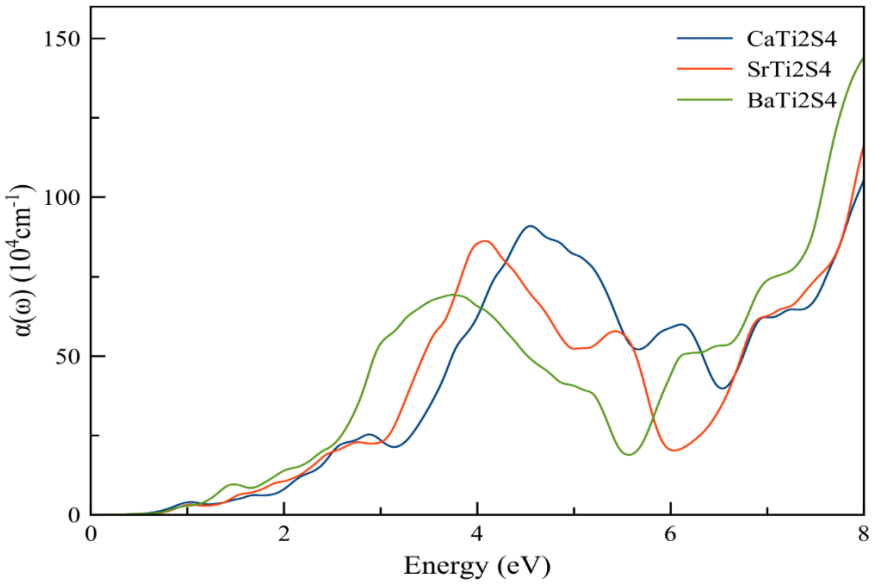

Figure 10. Calculated absorption coefficient as function of energy for ATi2S4 (A= Ca, Sr and Ba)

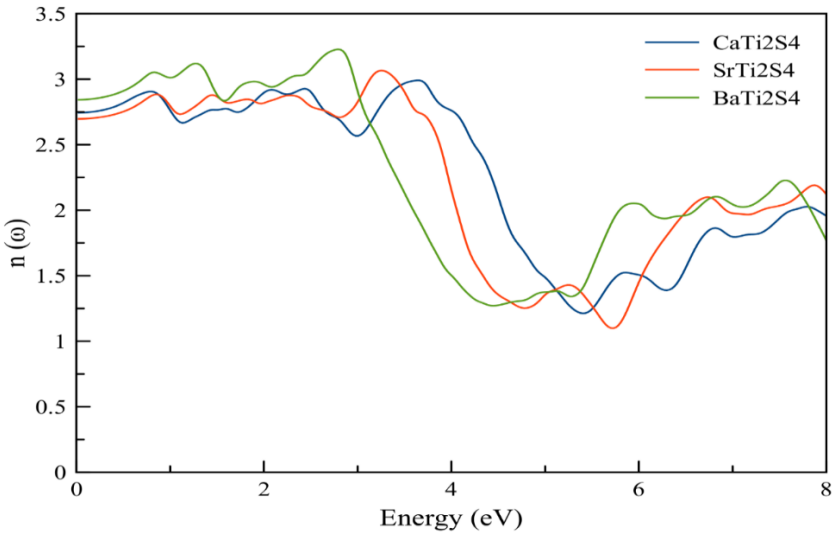

Figure 11. Calculated refractive index n(ω) as function of photon energy for ATi2S4 (A= Ca, Sr and Ba)

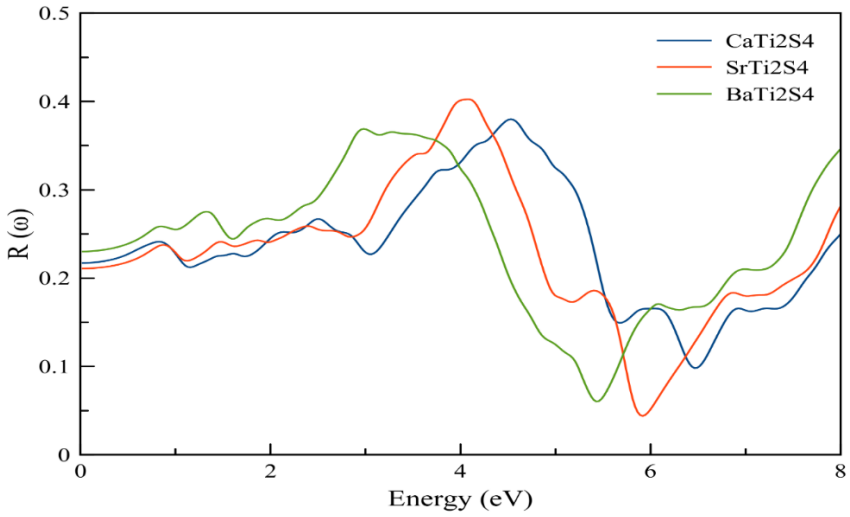

Figure 12. Calculated reflectivity spectra R(ω) as function of photon energy for ATi2S4 (A= Ca, Sr, Ba)

9. Conclusions

To summarize, we employed the FP-LAPW method using DFT in GGA and mBJ-GGA approximation to examine the structural, mechanical and elastic, electronic,magnetic and optical properties of spinel compounds consisting of ATi2S4 (A= Ca, Sr, Ba). Across all three compounds, their stable structures were of the FM type, and thus were more stable, both structurally and magnetically, than other potential structures.

Calculations of spin-polarized electronic band structure indicated that all ATi2S4 (A= Ca, Sr and Ba) compounds exhibit characteristics of ferromagnetic half-metallicity (HMF).

Demonstrating that our three compounds are half-metallic ferromagnetic, we can use the

Slater-Pauling rule which states that the total magnetic moment (M_{tot}), an integer valued at 8 μ_B, is equal to $M_{tot} = (Z_{tot} - 18)$ and Z_{tot} is the number of valence electrons.

Finally, The ATi2S4 spinel compounds have been observed to exhibit unique electronic and optical properties. Specifically, these materials have been found to display direct bandgap properties, meaning that the energy required to excite electrons across the bandgap is relatively low and corresponds to the absorption of light in the visible energy ranges. However, these materials also behave as indirect gap materials, which means that there are other, higher energy excitations that can occur within the material. This combination of direct and indirect bandgap behaviors makes these compounds highly attractive for optoelectronic devices, including single junction solar cells, where optimal absorption in the visible energy ranges is desirable for efficient energy conversion. These findings suggest that the ATi2S4 spinel compounds, with their unique electronic and optical properties, have promising applications in the field of optoelectronics.

References

[1] N. Grimes, Phys. Technol. 6 (1975) 22.

[2] M. Isobe, M. Arai, E. Takayama-Muromachi, J. Electron. Mater. 38 (2009) 1166.

[3] I. Žutić, J. Fabian, S. Das Sarma, Rev. Mod. Phys. 76 (2004) 323.

[4] M. Rana, S. P. Sanyal, Journal of Applied Physics 123 (2018) 194902.

[5] P. Hohenberg, W. Kohn, Phys. Rev. 136 (1964) B864.

[6] P. Blaha, K. Schwarz, G. K. H. Madsen, D. Kvasnicka, and J. Luitz, "WIEN2k, An Augmented Plane Wave + Local Orbitals Program for Calculating Crystal Properties," Vienna University of Technology, Austria, 2001

[7] J. P. Perdew, K. Burke, M. Ernzerhof, Phys. Rev. Lett. 77 (1996) 3865.

[8] P. Haas, F. Tran, P. Blaha, Phys. Rev. B 79 (2009) 209902.

[9] D. Koller, F. Tran, P. Blaha, Phys. Rev. B 85 (2012) 155109.

[10] G. K. Madsen, D. J. Singh, Comput. Phys. Commun. 175 (2006) 67-71.

[11] F. Birch, Phys. Rev. 71 (1947) 809.

[12] A. Mahmood, S.M. Ramay, W. Al-Masry, A.A. Al-Zahrani, N.Y.A. Al-Garadi, Mat.Res.Tech. 9 (2020) 14783.

[13] M. Jamal, M. Bilal, I. Ahmad, S. Jalali-Asadabadi, Journal of Alloys and Compounds 735 (2018) 569.

[14] M. J. Mehl, J. E. Osburn, D. A. Papaconstantopoulos, B. M. Klein, Phy. Rev. B 41 (1990) 10311.

[15] M. Born, “In on the Stability of Crystal Lattices”. Cambridge University Press, 1940, p. 160.

[16] M. Dacorogna, J. S. Ashkenazi, M. Peter, Phys. Rev. B 26 (1982) 1527.

[17] A. Q. Seh, D. C. Gupta, Int. J. Energy Res. 43 (2019) 8864.

[18] Z. Javdani, H. A. Badehian, H. Salehi, P. Amiri, Phys. Lett. A 378 (2014) 2644.

[19] H. Zaari, A.G. El Hachimi, A. Benyoussef, A. El Kenz, J. Magn. Magn Mater. 393 (2015) 183.

[20] D. J. Singh, Phys. Rev. B 82 (2010) 205102.

[21] M. Azzouz, Symmetry 9 (2017) 225.

[22] I. Galanakis, P. H. Dederichs, N. Papanikolaou, Phys. Rev. B 66 (2002) 134428.

[23] Magnetic Behavior of Diatomic Species - Chemistry LibreTexts", chem.libretexts.org, (Accessed 27 Jun. 2023).

[24] Silva FGD, Depeyrot J, Campos AFC, Aquino R, Fiorani D, Peddis D. Structural and Magnetic Properties of Spinel Ferrite Nanoparticles. J Nanosci Nanotechnol. 2019 Aug 1;19(8):4888-4902. doi:10.1166/jnn.2019.16877. PMID: 30913800. [25] B. Dec, R. Bogdanowicz, Photonic Letters of Poland 10 (2018) 39.

[26] J. Shiomi, K. Esfarjani, G. Chen, Phys. Rev. B 84 (2011) 104302.

[27] Y. Chen et al, Appl. Sci. 9 (2019) 620.

[28] D. R. Penn, Phys. Rev. 128 (1962) 5077.

[29] B. Amin, I. Ahmad, M. Maqbool, S. Goumri-Said, R. Ahmad, Journal of Applied Physics 109 (2011) 023109.